

LIBRARY
TECHNICAL REPORT SECTION
NAVAL POSTGRADUATE SCHOOL
MONTEREY, CALIFORNIA 93940

Technical Report No. 160 /

SACLANT ASW
RESEARCH CENTRE

ON THE CORRELATION FUNCTIONS IN TIME AND SPACE
OF WIND-GENERATED OCEAN WAVES

by

JAN GEERT DE BOER

15 DECEMBER 1969

VIALE SAN BARTOLOMEO, 400
I-19026-LA SPEZIA, ITALY

AD D865 249

[REDACTED]

TECHNICAL REPORT NO. 160

SACLANT ASW RESEARCH CENTRE
Viale San Bartolomeo 400
I 19026 - La Spezia, Italy

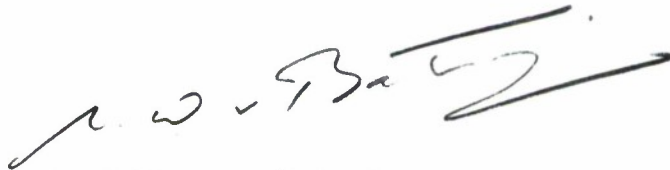
ON THE CORRELATION FUNCTIONS IN TIME AND SPACE
OF WIND-GENERATED OCEAN WAVES

By

Jan Geert de Boer


15 December 1969

APPROVED FOR DISTRIBUTION



Ir M.W. van Batenburg
Director

[REDACTED]



"A wind-generated sea is always short-crested."
"There is ample unexplored territory for anyone
with an interest in the statistical properties of
the short-crested sea."

B. Kinsman
[Ref.2, p.397]

Manuscript Completed:
1 December 1969




TABLE OF CONTENTS

	<u>Page</u>
LIST OF SYMBOLS	ii
ABSTRACT	1
ACKNOWLEDGEMENT	2
INTRODUCTION	3
1. STATISTICS OF THE OCEAN SURFACE	5
1.1 Introductory	5
1.2 Relations Between Surface Correlation Functions and Wave Spectra	7
1.3 The Sea-Surface Roughness Spectra	9
2. THE SURFACE CORRELATION FUNCTIONS IN TIME AND SPACE	13
3. THE TIME-CORRELATION FUNCTION	15
3.1 Introductory	15
3.2 The Neumann Spectrum	16
3.3 The Pierson-Moskowitz Spectrum	17
3.4 Discussion	17
4. THE SPACE-CORRELATION FUNCTION	21
4.1 Introductory	21
4.2 The Neumann Spectrum	22
4.3 The Pierson-Moskowitz Spectrum	26
4.4 Down-Wind and Cross-Wind Correlation	26
4.5 Discussion	29
CONCLUSIONS	32
APPENDIX A	
TOTAL ENERGY IN A FULLY DEVELOPED SEA	34
APPENDIX B	
CALCULATION OF THE INTEGRAL $I_1(\sigma, \vec{\rho})$	36
REFERENCES	

List of Figures

1. Time correlation function of wind-generated ocean surface waves.	16
2. Time auto-correlation function on a normalized scale	18
3. The functions $K_1(x)$ and $K_2(x)$.	24
4. Spatial correlation function of wind-generated ocean surface waves, derived from the Neumann spectrum.	25
5. The functions $L_1(x)$ and $L_2(x)$.	27
6. Spatial correlation function of wind-generated ocean surface waves, derived from the Pierson-Moskowitz spectrum.	28
7. Spatial correlation function of wind-generated ocean surface waves in the down-wind direction.	30
8. Spatial correlation function of wind-generated ocean surface waves in the cross-wind direction.	30
9. The difference between the spatial correlation functions of wind-generated ocean waves, obtained from the Neumann and the Pierson-Moskowitz spectra.	31

LIST OF SYMBOLS

A	constant
A^2	energy spectrum
B	constant
C, C'	constants
E	energy; mathematical expectation
F	correlation function
f	proportionality factor
g	acceleration due to gravity
h	standard deviation of surface roughness
J_0, J_1	Bessel functions
K	wave number; constant
N	correlation function of surface roughness
n	integer
p	real number
t	time
U	wind speed
X_1, X_2	orthogonal coordinates in horizontal plane
\vec{x}	position vector in horizontal plane
z	vertical dimension
α	constant
β	constant
γ	constant
δ	Dirac function
ζ	surface elevation
η	difference in X_2 -coordinates (cross-wind)
η_N	normalized η : $\eta_N = 2g\eta/U^2$

List of Symbols (Cont'd)

θ	wave direction with respect to average wind direction
ξ	difference in X_1 -coordinates (down-wind)
ξ_N	normalized ξ : $\xi_N = 2g\xi/U^2$
$\vec{\rho}$	difference vector in horizontal plane
ρ	modulus of $\vec{\rho}$
ρ_N	normalized ρ : $\rho_N = 2g\rho/U^2$
σ, σ'	radian frequency of surface waves
σ_0	normalizing frequency: $\sigma_0 = g/U$
σ_1	cut-off frequency
σ_M	frequency where Φ reaches its maximum
τ	time difference
τ_N	normalized τ : $\tau_N = \tau/U$
Φ	wave energy spectrum
φ	polar angle
Ψ	wave spectrum
ω	normalized radian frequency of surface waves

ON THE CORRELATION FUNCTIONS IN TIME AND SPACE
OF WIND-GENERATED OCEAN WAVES

By

Jan Geert de Boer

ABSTRACT

When wind-generated ocean surface waves are described statistically by means of a wave energy spectrum, the correlation function for the surface elevation at two points and two instants of time follows as an integral over the wave spectrum. The time-correlation function and the spatial-correlation function, which are important for the statistical description of an underwater sound field scattered from the sea surface, follow from this integral as special cases. They are examined here for two proposed spectra for fully-developed seas — the Neumann and the Pierson-Moskowitz spectra — by numerical integration.

It is shown that the spatial-correlation function, although a function of two variables, can be expressed in terms of two functions of only one variable each, when a cosine-squared law for the directionality of the wave spectrum is assumed. These functions are tabulated and plotted. A very simple relation is sufficient to reconstruct the entire anisotropic spatial correlation function from these basic functions.

ACKNOWLEDGEMENT

The study reported here was made when the author was a Summer Research Assistant at SACLANTCEN, working under the supervision of Mr Leonard Fortuin of the Sound Propagation Group. He wishes to thank Mr Fortuin for his advice and help, without which the study could not have been finished in the time available. The help of Dr M. Briscoe during the preparation and revision of this report is also appreciated.

INTRODUCTION

The subject of scattering and reflection of sound waves from rough boundaries, such as the sea surface, has received increasing interest in the past fifteen years. Many models, both of deterministic and random character, have been proposed to describe the scattering phenomenon. A detailed discussion of the existing literature can be found in Ref. 1.

The elevation and slopes of the sea surface are random processes in time and space. Consequently, a realistic description of the scattered sound field must also be stochastic in nature. Statistical quantities such as mean value, covariance and correlation are hence of interest; and, as they involve the statistics of the sea surface, knowledge of this boundary is required.

If the statistical description of the scattered field is limited to first and second moments, the sea surface is sufficiently characterized by mean value and covariance. Moreover, if the mean value is made zero, which can be done without loss of generality (the mean level does not change in the time interval that is typical for an acoustical experiment), it is only the correlation function of the surface that has to be known.

The most realistic way to obtain this correlation function is by using the (Neumann) theory of the surface wave spectrum for a fully-developed sea. This spectrum and the correlation function are related via the familiar Fourier transform.

Several formulae have been proposed for the spectrum of wind-generated ocean waves in a fully-developed sea. It is the aim of this report to compute the time-correlation function and

the spatial-correlation function for the two spectra proposed by Neumann and by Pierson and Moskowitz. It should be noted that the Neumann spectrum has now been discredited on both theoretical and experimental grounds, but it is included here for comparison and because it is so commonly referred to in the existing acoustic literature on scattering from the sea surface.

1. STATISTICS OF THE OCEAN SURFACE

1.1 Introductory

When wind is blowing over the surface of the sea, a very complicated mechanism of interaction between air and water causes the formation of surface waves. Many studies have been made to investigate this phenomenon, and many models have been proposed to describe it. But a description that covers all aspects is not yet available.

Attempts have been made to characterize the sea surface with only one parameter, especially the wind speed. But the time during which a certain constant wind has been blowing (the "duration") and the size of the area over which it has been blowing (the "fetch") also play an important role. This has lead to the concept of a "fully-developed sea", over which the wind speed and direction have been constant long enough for the wave system to contain the maximum amount of energy it can possibly have: an equilibrium has been reached. Clearly, this is only a theoretical construction: winds of constant speed and direction do not last very long, certainly not in large areas. Nevertheless, the idea of a "fully-aroused sea" has produced useful results.

A very good introduction to the subject is given by Kinsman [Ref. 2]. More recent insights are presented by Phillips [Ref. 3]. Both authors point out that the sea surface is a random process, in space as well as time. This process, $z = \xi(\vec{x}, t)$, is not Gaussian (there is a certain skewness of the waves, and waves of infinite height have zero probability), but in many respects it may be considered as "quasi-Gaussian", as measurements have indicated.

In its most general form the second moment of the process is the correlation function

$$F = E [\zeta(\vec{x}_1, t_1) \zeta(\vec{x}_2, t_2)] . \quad [\text{Eq. 1}]$$

In principle it depends on the position of the points of observation and on the observation times. But the assumption that the sea surface is homogeneous (at least in the area where an experiment takes place) and stationary (at least for the duration of an experiment) reduces the correlation function to a function of only space differences and time differences:

$$\begin{aligned} E [\zeta(\vec{x}_1, t_1) \zeta(\vec{x}_2, t_2)] &\equiv E [\zeta(\vec{x}_1, t_1) \zeta(\vec{x}_1 + \vec{\rho}, t_1 + \tau)] \\ &= F(\vec{\rho}, \tau) , \end{aligned} \quad [\text{Eq. 2}]$$

where

$$\vec{\rho} = \vec{x}_2 - \vec{x}_1 \quad \text{and} \quad \tau = t_2 - t_1 . \quad [\text{Eq. 3}]$$

In the past it has sometimes been assumed that the spatial-correlation function of the sea surface had the shape of a Gaussian curve, but this assumption has turned out to be incorrect and unsatisfactorily. "The most realistic way to incorporate the correlation function of surface height and slopes is via the theory of the surface wave spectrum" [Ref. 1, p.91].

According to this theory the sea surface is considered as the combined effect of a large band of sinusoidal surface waves that travel over the surface in very many directions, each having its own speed and hence its own wave number. In this way the idea of a surface wave energy spectrum has been formed.

Many waves travel in the direction of the mean wind. But waves are also generated sideways, at least in the angular interval $(-\pi/2, \pi/2)$, and may be even in an interval $(-\pi, \pi)$, because of non-linear wave interactions. It can be said, however, that waves are generally strongest in the down-wind direction. Hence the sea surface is anisotropic, and the wave spectrum depends

not only on frequency or wave number, but also on direction.

1.2 Relations Between Surface Correlation Functions and Wave Spectra

In its most general form the surface correlation function deals with the surface elevation at two different points and at two different instants of time. Other correlation functions can be derived from it by taking the time difference equal to zero, by considering coinciding points, or by assuming the surface to be isotropic. For each correlation function obtained in this way a corresponding spectral function can be defined via a Fourier transform relation. These relations are discussed in detail in Refs. 2 and 3.

Returning to Eq. 2, we normalize F :

$$F(\vec{\rho}, \tau) = h^2 N(\vec{\rho}, \tau), \quad [\text{Eq. 4}]$$

$$h^2 = F(0,0); \quad [\text{Eq. 5}]$$

the vector $\vec{\rho}$ has components ξ and η , in the X_1 and X_2 directions respectively.

The correlation function $N(\vec{\rho}, \tau)$ is the three-dimensional Fourier transform of the most general wave spectrum $\Psi(\vec{K}, \sigma)$, a function of both wave number and frequency:

$$h^2 N(\vec{\rho}, \tau) = \iiint_{-\infty}^{\infty} d\vec{K} \int_{-\infty}^{\infty} d\sigma' \Psi(\vec{K}, \sigma') \exp[i(\vec{K} \cdot \vec{\rho} - \sigma' \tau)]. \quad [\text{Eq. 6}]$$

For small-amplitude, deep-water waves there is a unique relation between the wave number and the frequency: the dispersion relation

$$K = \sigma^2/g. \quad [\text{Eq. 7}]$$

This implies [Refs. 2 and 3] that

$$\Psi(\vec{K}, \sigma') = \Psi(\vec{K}) \delta(\sigma - \sigma'), \quad [\text{Eq. 8}]$$

so that

$$h^2 N(\vec{\rho}, \tau) = \iint_{-\infty}^{\infty} d\vec{K} \Psi(\vec{K}) \exp[\vec{K} \cdot \vec{\rho} - \sigma \tau] \quad [\text{Eq. 9}]$$

follows. With polar coordinates (K, θ) and again the dispersion relation, we then find

$$h^2 N(\xi, \eta) = \int_{-\pi}^{\pi} d\theta \int_0^{\infty} d\sigma \frac{2\sigma^3}{g^2} [\Psi(K, \theta)]_{K=\sigma^2/g} \cdot \exp \left[i \frac{\sigma^2}{g} (\xi \cos \theta + \eta \sin \theta) - i\sigma\tau \right]. \quad [\text{Eq. 10}]$$

Putting

$$\Phi(\sigma, \theta) = \frac{4\sigma^3}{g^2} [\Psi(K, \theta)]_{K=\sigma^2/g} \quad [\text{Eq. 11}]$$

into Eq. 10, and realizing that N is a real function, we get finally:

$$N(\xi, \eta, \tau) = (2h^2)^{-1} \int_{-\pi}^{\pi} d\theta \int_0^{\infty} d\sigma \Phi(\sigma, \theta) \cos \left[\frac{\sigma^2}{g} (\xi \cos \theta + \eta \sin \theta) - \sigma\tau \right]. \quad [\text{Eq. 12}]$$

This formula is the starting point for our calculations. It may be compared with Ref. 2[p.378, Eq.(8.3:3)].

The spectral function $\Phi(\sigma, \theta)$ is non-negative over the entire (σ, θ) - plane. The integral

$$I = \int_{\theta_1}^{\theta_2} d\theta \int_{\sigma_1}^{\sigma_2} d\sigma \Phi(\sigma, \theta) \quad [\text{Eq. 13}]$$

gives a measure of the energy in the wave field having frequencies between σ_1 and σ_2 , and travelling in directions between θ_1 and θ_2 . If we integrate the spectrum over the whole (σ, θ) -plane, we have an estimate of the total energy in the wave field:

$$E = \int_{-\pi}^{\pi} d\theta \int_0^{\infty} d\sigma \Phi(\sigma, \theta) . \quad [\text{Eq. 14}]$$

1.3 The Sea-Surface Roughness Spectra

Most oceanographic literature about the surface wave spectra deals with the function $\Phi(\sigma)$, rather than with $\Phi(\sigma, \theta)$. They are related as follows:

$$\Phi(\sigma) = \int_{-\pi}^{\pi} d\theta \Phi(\sigma, \theta) . \quad [\text{Eq. 15}]$$

When $\Phi(\sigma)$ is given and $\Phi(\sigma, \theta)$ is needed, an inverse relation is required.

There is some disagreement in the literature about the explicit form of the function $\Phi(\sigma)$. Part of the discrepancies can be explained if we realize that the measurements on which the empirical formulae for $\Phi(\sigma)$ are based have not all been made in seas with the same state of development [Ref. 1, p.88-89].

A formerly-used estimate for the functional form of $\Phi(\sigma)$ is:

$$\Phi(\sigma) = \frac{\pi}{2} C \sigma^{-6} \exp(-2g^2 \sigma^{-2} U^{-2}) , \quad [\text{Eq. 16}]$$

where $C = 3.05 \text{ m}^2/\text{s}^5$. This is the Neumann spectrum, usually called $A^2(\sigma)$ [see Ref. 2, p. 389]. Its anisotropic version is given by Pierson, Neumann and James [see Ref. 2, p.399]:

$$\begin{aligned} \Phi(\sigma, \theta) \equiv A^2(\sigma, \theta) &= C \sigma^{-6} \exp(-2g^2 \sigma^{-2} U^{-2}) \cos^2 \theta \\ &\text{for } \sigma_1 \leq \sigma < \infty, \quad |\theta| \leq \frac{\pi}{2}, \\ &= 0, \text{ otherwise.} \end{aligned} \quad [\text{Eq. 17}]$$

Comparison between Eqs. 16 and 17 yields a relation between the anisotropic spectrum and its reduced form, which will also be used for other spectra:

$$\begin{aligned} \Phi(\sigma, \theta) &= \frac{2}{\pi} \Phi(\sigma) \cos^2 \theta & \left(\begin{array}{l} \sigma_1 \leq \sigma < \infty, \\ |\theta| \leq \pi/2 \end{array} \right) \\ &= 0, \text{ otherwise}^*. \end{aligned} \quad [\text{Eq. 18}]$$

Another spectral function is mentioned by Schulkin [Ref. 4]; it has a sharp low-frequency cut off:

$$\begin{aligned} \Psi(K, \theta) &= \frac{2}{\pi} \Psi(K) \cos^2 \theta & \text{for } |\theta| \leq \frac{\pi}{2} \\ &= 0 & \text{for } |\theta| > \frac{\pi}{2} \end{aligned} \quad [\text{Eq. 19}]$$

with

$$\Psi(K) = \int_0^{2\pi} d\theta \Psi(K, \theta) \quad [\text{Eq. 20}]$$

$$\begin{aligned} &= BK^{-4} & \text{for } |K| \geq g U^{-2} \\ &= 0 & \text{for } |K| < g U^{-2}; \end{aligned} \quad [\text{Eq. 21}]$$

this is the Burling-Phillips spectrum.

The dimensionless constant B equals 0.46×10^{-2} according to Schulkin, and 0.6×10^{-2} according to Phillips [Ref. 3].

The expression for $\Phi(\sigma)$, as given by Neumann [Eq. 16], is most often met in the literature. But its asymptotic behaviour at high frequencies, showing a proportionality with σ^{-6} , has been

* Cox and Munk, and Wong, have found from ratios of up-wind to cross-wind mean square slopes that the cosine-squared law is too narrow to describe the directionality of the wind waves (see Ref. 4, p.17). We note in passing that the quantity "mean-square slope" is an important measure of sea surface roughness; it includes the roughness contribution of the small wave patches riding atop the large sea waves, which are important for acoustics and radar.

proved wrong. Pierson and Moskowitz [Ref. 5] gave arguments in favour of a σ^{-5} behaviour. They stated that "within the present limitation of data, the spectrums of fully developed wind-generated seas for winds measured at 19.5 metres are given very nearly by" [Ref. 5, p.5190]:

$$\Phi(\sigma) = \alpha g^2 \sigma^{-5} \exp \left[-\beta \left(\frac{\sigma_0}{\sigma} \right)^4 \right], \quad [\text{Eq. 22}]$$

with $\alpha = 8.10 \times 10^{-3}$, $\beta = 0.74$ and $\sigma_0 = g/U$, where U is the wind speed reported by the weather ships.

A formula in which the wind speed does not appear, and that also has a high-frequency behaviour of the type σ^{-5} , has been suggested by Phillips [Ref. 3]. He gave the formula

$$\Phi(\sigma) = C' g^2 \sigma^{-5}, \quad [\text{Eq. 23}]$$

where $C' = 1.2 \times 10^{-2}$, a dimensionless constant, that varies slightly with fetch.

In this report we will concentrate on two spectra, both proposed for a fully-aroused sea, namely the spectra given in Eq. 16 (Neumann) and Eq. 22 (Pierson-Moskowitz). Since the anisotropic version is required, we will also apply Eq. 18, with $\sigma_1 = 0$.

The frequencies σ_M , at which the energy spectra reach their maximum, and the maxima themselves, can be found easily. We have:

a) Neumann Spectrum

$$\sigma_M = \frac{g}{U} \sqrt{2/3} = 0.816 \frac{g}{U}, \quad [\text{Eq. 24}]$$

$$\Phi(\sigma_M) = f U^6; \quad [\text{Eq. 25}]$$

b) Pierson-Moskowitz Spectrum

$$\sigma_M = \frac{g}{U} \left(\frac{4\beta}{5} \right)^{\frac{1}{4}} = 0.877 \frac{g}{U} \quad [\text{Eq. 26}]$$

$$\Phi(\sigma_M) = f U^5. \quad [\text{Eq. 27}]$$

We see that with increasing wind speed σ_M decreases and $\Phi(\sigma_M)$ increases. For the surface wave spectrum this means more low frequencies and so a larger correlation distance.

A fully-developed sea for a fixed wind speed U is one whose spectrum contains components of all frequencies $0 \leq \sigma < \infty$, each with the maximum energy of which it is capable under the given wind. The total energy in such a sea is [cf Eqs. 14 and 15]

$$E = \int_0^{\infty} d\sigma \Phi(\sigma) = 2h^2. \quad [\text{Eq. 28}]$$

So we get for the spectra under study:

a) Neumann Spectrum

$$E = 3 C \left(\frac{\pi}{2} \right)^{3/2} \left(\frac{U}{2g} \right)^5; \quad [\text{Eq. 29}]$$

b) Pierson-Moskowitz Spectrum

$$E = \frac{4\alpha g^2}{\beta} \left(\frac{U}{2g} \right)^4. \quad [\text{Eq. 30}]$$

Details of the calculation can be found in Appendix A.

2. THE SURFACE CORRELATION FUNCTIONS IN TIME AND SPACE

The foregoing discussion of the surface wave spectra, and the relation between the directional spectrum and its reduced form, enable us to rewrite the formula for the surface correlation function $N(\vec{\rho}, \tau)$. From Eqs. 12 and 18, with $\sigma_1 = 0$, we obtain:

$$h^2 N(\vec{\rho}, \tau) = \frac{1}{\pi} \int_{-\pi/2}^{\pi/2} d\theta \int_0^\infty d\sigma \Phi(\sigma) \cos^2 \theta \cos \left[\frac{\sigma^2}{g} (\xi \cos \theta + \eta \sin \theta) - \sigma \tau \right] \quad [\text{Eq. 31}]$$

The normalized time-correlation function $N(0, \tau)$, and the normalized spatial-correlation function $N(\vec{\rho}, 0)$ follow immediately from this expression. They will be calculated in the following sections.

For computational reasons we bring Eq. 31 into a more convenient form: we divide by h^2 , change the order of integration, and separate the variables in the argument of the second cosine function. Then we get:

$$N(\vec{\rho}, \tau) = (\pi h^2)^{-1} \left[\int_0^\infty d\sigma \Phi(\sigma) \cos(\sigma \tau) I_1(\sigma, \vec{\rho}) + \int_0^\infty d\sigma \Phi(\sigma) \sin(\sigma \tau) I_2(\sigma, \vec{\rho}) \right] \quad [\text{Eq. 32}]$$

with

$$I_1(\sigma, \vec{\rho}) = \int_{-\pi/2}^{\pi/2} d\theta \cos^2 \theta \cos \left[\frac{\sigma^2}{g} (\xi \cos \theta + \eta \sin \theta) \right] \quad [\text{Eq. 33a}]$$

$$I_2(\sigma, \vec{\rho}) = \int_{-\pi/2}^{\pi/2} d\theta \cos^2 \theta \sin \left[\frac{\sigma^2}{g} (\xi \cos \theta + \eta \sin \theta) \right] \quad [\text{Eq. 33b}]$$

We may note in passing that h^2 can be calculated with Eq. 28:

$$h^2 = \frac{1}{2} \int_0^\infty d\sigma \Phi(\sigma) = \frac{1}{2} E, \quad [\text{Eq. 34}]$$

an expression that follows also from Eq. 31 by putting $\xi = \eta = 0$, and $\tau = 0$. The quantities E for the Neumann spectrum and the Pierson-Moskowitz spectrum are given in Eqs. 29 and 30, respectively. Hence we find for h^2 :

a) Neumann Spectrum

$$h^2 = \frac{3}{2} C \left(\frac{\pi}{2}\right)^{3/2} \left(\frac{U}{2g}\right)^5 \quad [\text{Eq. 35}]$$

with $C = 3.05$;

b) Pierson-Moskowitz Spectrum

$$h^2 = \frac{2\alpha g^2}{\beta} \left(\frac{U}{2g}\right)^4, \quad [\text{Eq. 36}]$$

with $\alpha = 8.10 \times 10^{-3}$, $\beta = 0.74$.

3. THE TIME-CORRELATION FUNCTION

3.1 Introductory

The correlation function $N(\vec{\rho}, \tau)$ given in Eq. 32 is too general for a detailed analysis. In this section we want to study its behaviour as a time-correlation function. Experimentally, this function could be obtained by observing the wave pattern at only one point, but for a long time. The time record from a shipborne wave height meter, or from a wavepole [both giving an estimate of $\zeta(t)$] could serve as the raw data. The function $N(0, \tau)$ could then be calculated approximately with the formula

$$N(0, \tau) = \frac{1}{T} \int_{t_0}^{t_0+T} dt \zeta(t) \zeta(t + \tau) . \quad [\text{Eq. 37}]$$

From the theoretical side, as is our concern in this report, $N(0, \tau)$ for a fully-developed sea follows from Eqs. 32 and 33 by setting $\vec{\rho} = 0$, i.e. $\xi = \eta = 0$. We then have

$$N(0, \tau) = (\pi h^2)^{-1} \int_0^\infty d\sigma \Phi(\sigma) \cos(\sigma\tau) I_1(\sigma, 0) , \quad [\text{Eq. 38}]$$

with

$$I_1(\sigma, 0) = \int_{-\pi/2}^{\pi/2} d\theta \cos^2 \theta . \quad [\text{Eq. 39}]$$

But the integral I_1 is easily evaluated; its value is $\pi/2$. And so we have finally

$$N(0, \tau) = (2h^2)^{-1} \int_0^\infty d\sigma \Phi(\sigma) \cos(\sigma\tau) , \quad [\text{Eq. 40}]$$

which says that $N(0, \tau)$ is the Fourier cosine transform of $\Phi(\sigma)$.

3.2 The Neumann Spectrum

In Eq. 40 we have to substitute the energy spectrum given by Eq. 16, and the value for h^2 from Eq. 35. The final result can be written in a more convenient form if we introduce the variable

$$z = \frac{U^2 \sigma^2}{2g^2}, \quad [\text{Eq. 41}]$$

and normalize the time delay τ by:

$$\tau_N = \tau/U. \quad [\text{Eq. 42}]$$

We note in passing that a similar normalization can be found in Ref. 5.

With these modifications we get:

$$N(0, \tau_N) = \frac{4}{3\sqrt{\pi}} \int_0^\infty dz z^{-3\frac{1}{2}} \exp(-\frac{1}{z}) \cos(g\sqrt{2} \sqrt{z} \tau_N). \quad [\text{Eq. 43}]$$

Clearly the wind speed U does not influence the shape of the curve, but only the time scale.

Unfortunately, we have not been able to solve this integral analytically. Hence, a numerical integration has been performed. The result is plotted in Fig. 1.

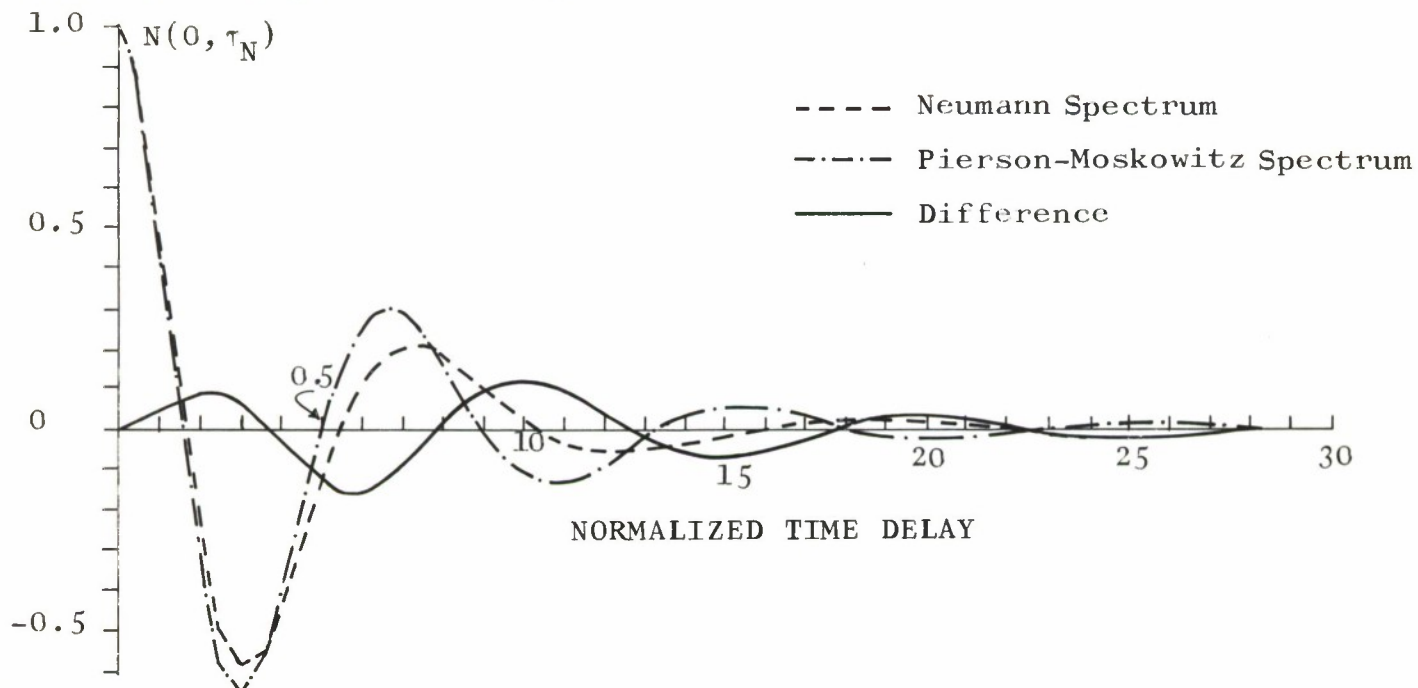


FIG. 1 TIME CORRELATION FUNCTION OF WIND-GENERATED OCEAN SURFACE WAVES
The normalized time equals U^{-1} times the actual time

It should be noted that, although $N(0, \tau)$ and $\Phi(\sigma)$ are related via the familiar Fourier cosine transform [Eq. 40], common numerical techniques such as the fast Fourier transform (FFT) cannot be used. This is because the FFT requires an equidistant sampling of $\Phi(\sigma)$, which is not suitable for this function since it has a steep rising part ($0 \leq \sigma \leq \sigma_M$) and a very slowly descending part ($\sigma_M \leq \sigma < \infty$).

3.3 The Pierson-Moskowitz Spectrum

In this case the spectrum of Eq. 22 and h^2 of Eq. 36 have to be substituted into Eq. 40. This time we change from σ to the variable

$$z = \beta(\sigma_0/\sigma)^4; \quad [\text{Eq. 44}]$$

the result is

$$N(0, \tau_N) = \int_0^\infty dz \exp(-z) \cos(\beta^{\frac{1}{4}} g \tau_N z^{-\frac{1}{4}}), \quad [\text{Eq. 45}]$$

again with $\tau_N = \tau/U$. This integral has also been approximated numerically. The result is presented in Fig. 1, together with its deviation from the Neumann curve.

3.4 Discussion

In Ref. 6, Latta and Bailie used very sophisticated mathematical techniques to calculate analytically the Fourier cosine transform of the energy spectrum [see Eq. 40] for the Neumann and the Pierson-Moskowitz spectra. The resulting formulae are so complicated, however, that they also had to use a computer for the final evaluation of the function $N(0, \tau)$. Figure 2 shows a copy of their curves, for comparison with Fig. 1; it also includes a curve found by Bendat [Ref. 7], for the Pierson-Moskowitz spectrum.

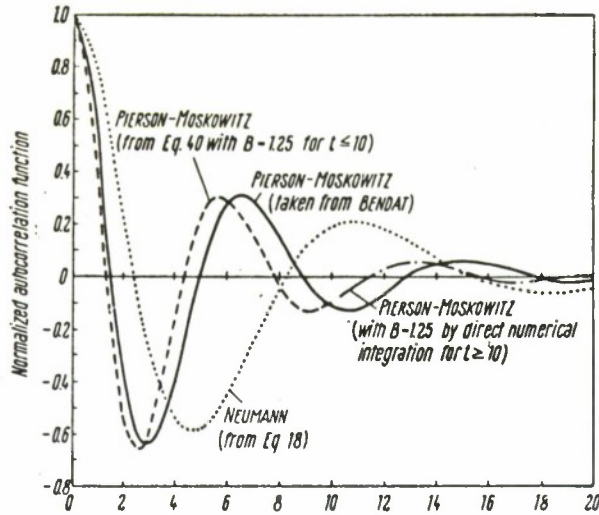


FIG. 2 TIME AUTO-CORRELATION FUNCTIONS ON A NORMALIZED SCALE (From Ref. 6)

Unfortunately, Latta and Bailie plotted their results on a normalized time scale, without giving explicitly the normalization factor, so that a quantitative comparison between their curves and ours becomes quite difficult.

The first thing we notice, when comparing Figs. 1 and 2, is that if we multiply our time scale by ten, our PM-curve is in good agreement with that of Bendat, who used a very simple integrating routine. Because the Latta-Bailie curve is only slightly different (their result is probably more accurate, since their calculation is far more rigorous than Bendat's and ours), we might conclude that they have normalized the time scale in accordance with Ref. 5 [p.5182], i.e. using $\tau_N = g\tau/U$. However this would include a normalized frequency $\omega = \frac{\sigma U}{g}$ and Eq. 22 would then change into (in the notation of Ref. 6)

$$\Phi(\omega) = AB \omega^{-5} \exp(-B\omega^{-4}), \quad [\text{Eq. 46}]$$

with

$$A = \frac{\alpha}{\beta} \frac{U^5}{g^3}, \quad B = \beta = 0.74. \quad [\text{Eq. 47}]$$

Nevertheless, Fig. 2 gives the value $B = 1.25$. Hence, $\tau_N = g\tau/U$, or $\tau_N = \tau/\gamma U$ with $\gamma = 0.1020$, does not seem to be the

normalization formula used, but it is very close to it. Indeed, if we solve the equation

$$\beta \left(\frac{g}{U\sigma} \right)^4 = B \omega^{-4} \quad [\text{Eq. 48}]$$

we obtain

$$\omega = \left(\frac{B}{\beta} \right)^{\frac{1}{4}} \frac{U\sigma}{g}, \quad [\text{Eq. 49}]$$

and with $B = 1.25$, $\beta = 0.74$ and $g = 9.81$ this gives

$$\omega = \gamma U\sigma, \quad A = \gamma \frac{\alpha}{\beta} \frac{U^5}{g^2}, \quad [\text{Eq. 50}]$$

with $\gamma = 0.1165$. Figures 1 and 2 can hence be compared if we multiply our scale by $\gamma^{-1} = 8.6$. A difference between the curves from the Neumann spectrum is then apparent, and this discrepancy is hard to explain, because of lack of information. First we note that Latta and Bailie have also normalized the Neumann-spectrum [Eq. 16]; they wrote

$$\Phi(\omega) = K \omega^{-6} \exp(-A \omega^2). \quad [\text{Eq. 51}]$$

The parameter A has not been defined. With $\omega = \gamma U\sigma$ we would get

$$A = 2\gamma^2 g^2 = 2 \left(\frac{B}{\beta} \right)^{\frac{1}{2}}, \quad [\text{Eq. 52}]$$

which is not in agreement with Eq. 50. This leads us to the conclusion that the symbol A has been used for two completely different quantities.

In the final formula for $N(0, \tau)$, calculated for the Neumann-spectrum [Ref. 6], the parameter A appears again, as it should:

$$N(0, \tau) = \frac{8}{3} \sqrt{\pi} \sum_{n=0}^{\infty} \frac{(-1)^n \left(\frac{n-1}{2} \right) \left(\frac{n-3}{2} \right) A^{\frac{n}{2}} \tau^n}{\Gamma(n+1) \Gamma \left(\frac{n+1}{2} \right)}. \quad [\text{Eq. 53}]$$

Nevertheless, in Fig. 2 a curve is plotted without a value assigned to A .

For all these reasons we shall not attempt a quantitative comparison between Figs. 1 and 2, as far as the Neumann curve is concerned. We only conclude that the curves show a similar behaviour.

The fact that the time scale in Fig. 1 could be normalized by dividing the real time delay by the wind speed is very interesting. It means that a fully-developed sea does not change its shape, but only its scale, when the wind speed is changed and a new equilibrium has been reached. The whole wave pattern, in a statistical sense, is stretched when the wind speed increases and contracted when it decreases. A fetch of infinite length and a constant wind of infinite duration are essential for this interpretation.

4. THE SPACE-CORRELATION FUNCTION

4.1 Introductory

When sound waves are scattered from the sea surface not one point, but a whole surface area, is involved. This explains why the spatial-correlation function $N(\vec{\rho}, 0)$ is important for the description of the scattered sound field. In fact, its importance is far greater than that of $N(0, \tau)$.

Experimentally $N(\vec{\rho}, 0)$ is hard to obtain. In principle, its calculation requires the surface elevation in a large area, at one instant of time, i.e. $\zeta(\vec{x}, t)$ for $t=t_0$ and \vec{x} ranging through a certain area A large enough to include the biggest $\vec{\rho}$ of interest. Given this information, $N(\vec{\rho}, 0)$ could then be computed with the formula

$$N(\vec{\rho}, 0) = \frac{1}{A} \iint d\vec{x} \zeta(\vec{x}, t_0) \zeta(\vec{x} + \vec{\rho}, t_0). \quad [\text{Eq. 54}]$$

An approximation made using a set of sample positions $\vec{x}_{i,j}$ is also possible:

$$N(\vec{\rho}_{\ell,m}, 0) \approx \frac{1}{PQ} \sum_{i=1}^P \sum_{j=1}^Q \zeta(\vec{x}_{i,j}, t_0) \zeta(\vec{x}_{i+\ell, j+m}, t_0), \quad [\text{Eq. 55}]$$

where $\vec{\rho}_{\ell,m} = \vec{x}_{i+\ell, j+m} - \vec{x}_{i,j}$. This would require PQ wave-height meters, whose positions are fixed and well known, and a synchronous recording of their readings. Such an experiment is hard to imagine.

More promising seems the optical method described by Stilwell [Ref. 8], in which the sea surface is illuminated by a "continuous skylight" and recorded photographically. Such a record indeed

represents a continuous surface area at one instant of time. The data processing is quite simple. "By the use of optical analysis it is possible to resolve the variations of density in the surface. When a transparency of a surface photograph is placed in one focal plane of a lens, the Fourier transform of the variations appear as light amplitude in the other focal plane. This information, in addition to the height and aspect angle of the camera, allows the energy spectrum of the surface to be obtained". [Ref. 8, Abstract].

When the surface wave spectrum is given, as in our case, $N(\vec{\rho}, 0)$ can be calculated from Eqs. 32 and 33 by taking $\tau = 0$. Doing so we get

$$N(\vec{\rho}, 0) = (\pi h^2)^{-1} \int_0^\infty d\sigma \, \Phi(\sigma) I_1(\sigma, \vec{\rho}) \quad [\text{Eq. 56}]$$

with

$$I_1(\sigma, \vec{\rho}) = \int_{-\pi/2}^{\pi/2} d\theta \cos^2 \theta \cos \left[\frac{\sigma^2}{g} (\xi \cos \theta + \eta \sin \theta) \right]. \quad [\text{Eq. 57}]$$

The integral I_1 can be expressed in terms of Bessel functions [see Appendix B for details]:

$$I_1(\sigma, \vec{\rho}) = \pi \rho^{-2} \left[\xi^2 J_0\left(\rho \frac{\sigma^2}{g}\right) + (\eta^2 - \xi^2) \left(\rho \frac{\sigma^2}{g}\right)^{-1} J_1\left(\rho \frac{\sigma^2}{g}\right) \right]. \quad [\text{Eq. 58}]$$

4.2 The Neumann Spectrum

In Eq. 56 we substitute Eqs. 58, 16 and 35. Moreover, we introduce a normalized correlation distance $\vec{\rho}_N$, with components ξ_N and η_N , by using the relation [cf Ref. 5, p.5182]:

$$\vec{\rho}_N = \frac{2g}{U^2} \vec{\rho}, \quad [\text{Eq. 59}]$$

and change the variable σ by taking, as in Sect. 3.2:

$$z = \frac{\sigma^2 U^2}{2g^2}. \quad [\text{Eq. 60}]$$

Then the correlation function $N(\vec{\rho}, 0)$ can be written in Cartesian coordinates (with $\rho_N = \sqrt{\xi_N^2 + \eta_N^2}$), as:

$$N(\xi_N, \eta_N, 0) = \rho_N^{-2} \left[\xi_N^2 K_1(\rho_N) + (\eta_N^2 - \xi_N^2) K_2(\rho_N) \right], \quad [\text{Eq. 61}]$$

or in polar coordinates ($\xi_N = \rho_N \cos \varphi$, $\eta_N = \rho_N \sin \varphi$) as:

$$N(\rho_N, \varphi, 0) = \cos^2 \varphi K_1(\rho_N) + (\sin^2 \varphi - \cos^2 \varphi) K_2(\rho_N), \quad [\text{Eq. 62}]$$

where

$$K_1(\rho_N) = \frac{8}{3\sqrt{\pi}} \int_0^\infty dz e^{-1/z} z^{-7/2} J_0(\rho_N z) \quad [\text{Eq. 63a}]$$

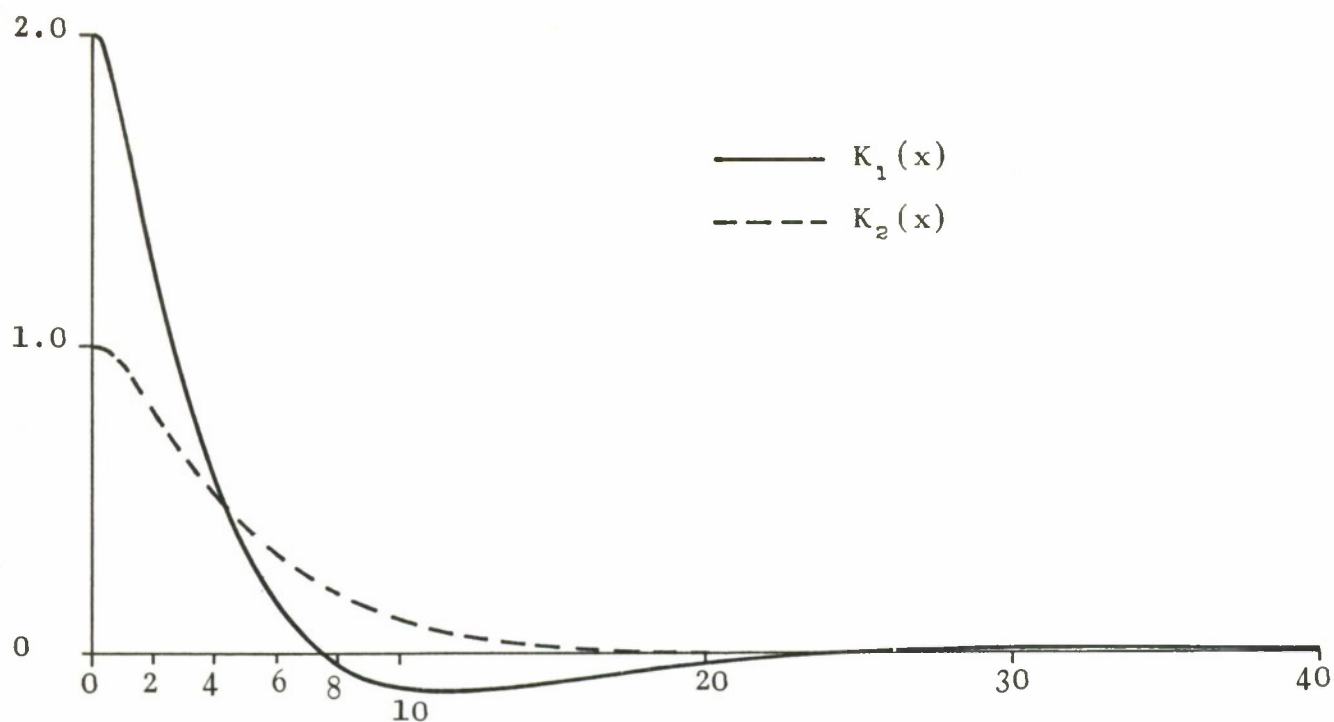
$$K_2(\rho_N) = \frac{8}{3\sqrt{\pi}} \int_0^\infty dz e^{-1/z} z^{-7/2} \frac{J_1(\rho_N z)}{(\rho_N z)}. \quad [\text{Eq. 63b}]$$

The functions K_1 and K_2 have been calculated numerically, on a digital computer (Elliott 503), and are plotted in Fig. 3. For later use their sample values are given in Table 1. The fact that they are one-dimensional simplifies the calculation of the two-dimensional function $N(\xi_N, \eta_N, 0)$ considerably: we only need to read the values of K_1 and K_2 into the computer, after which Eqs. 61 or 62 enables us to compute any value of the surface $N(\xi_N, \eta_N, 0)$. Moreover, N is symmetric with respect to the diagonal $\xi_N = \eta_N$:

$$N(\xi_N, \eta_N, 0) = N(\eta_N, \xi_N, 0); \quad [\text{Eq. 64}]$$

this halves the number of samples to be computed.

In Fig. 4 we have plotted the correlation function $N(\xi_N, \eta_N, 0)$ for the Neumann spectrum. The scales are normalized by using Eq. 59.



NORMALIZED CORRELATION DISTANCE

FIG. 3 THE FUNCTIONS $K_1(x)$ AND $K_2(x)$

x	$K_1(x)$	$K_2(x)$
0	2.000000	1.000000
1	1.723824	0.922369
2	1.295799	0.788175
3	0.902805	0.650454
4	0.585233	0.525517
5	0.344280	0.418094
6	0.169415	0.328420
7	0.047631	0.254962
8	-0.033259	0.195599
9	-0.083592	0.148139
10	-0.111697	0.110546
11	-0.124076	0.081028
12	-0.125690	0.058053
13	-0.120249	0.040338
14	-0.110477	0.026820
15	-0.098337	0.016631
16	-0.085208	0.009063
17	-0.072035	0.003545
18	-0.059438	-0.000382
19	-0.047799	-0.003083
20	-0.037332	-0.004850
21	-0.028127	-0.005914
22	-0.020191	-0.006456
23	-0.013475	-0.006618
24	-0.007892	-0.006509
25	-0.003340	-0.006215
26	0.000295	-0.005800
27	0.003128	-0.005314
28	0.005268	-0.004792
29	0.006819	-0.004260
30	0.007875	-0.003739
31	0.008521	-0.003240
32	0.008834	-0.002773
33	0.008882	-0.002343
34	0.008723	-0.001951
35	0.008408	-0.001600
36	0.007978	-0.001288
37	0.007468	-0.001013
38	0.006905	-0.000774
39	0.006314	-0.000567
40	0.005712	-0.000391

TABLE 1 SAMPLE VALUES OF K_1 AND K_2

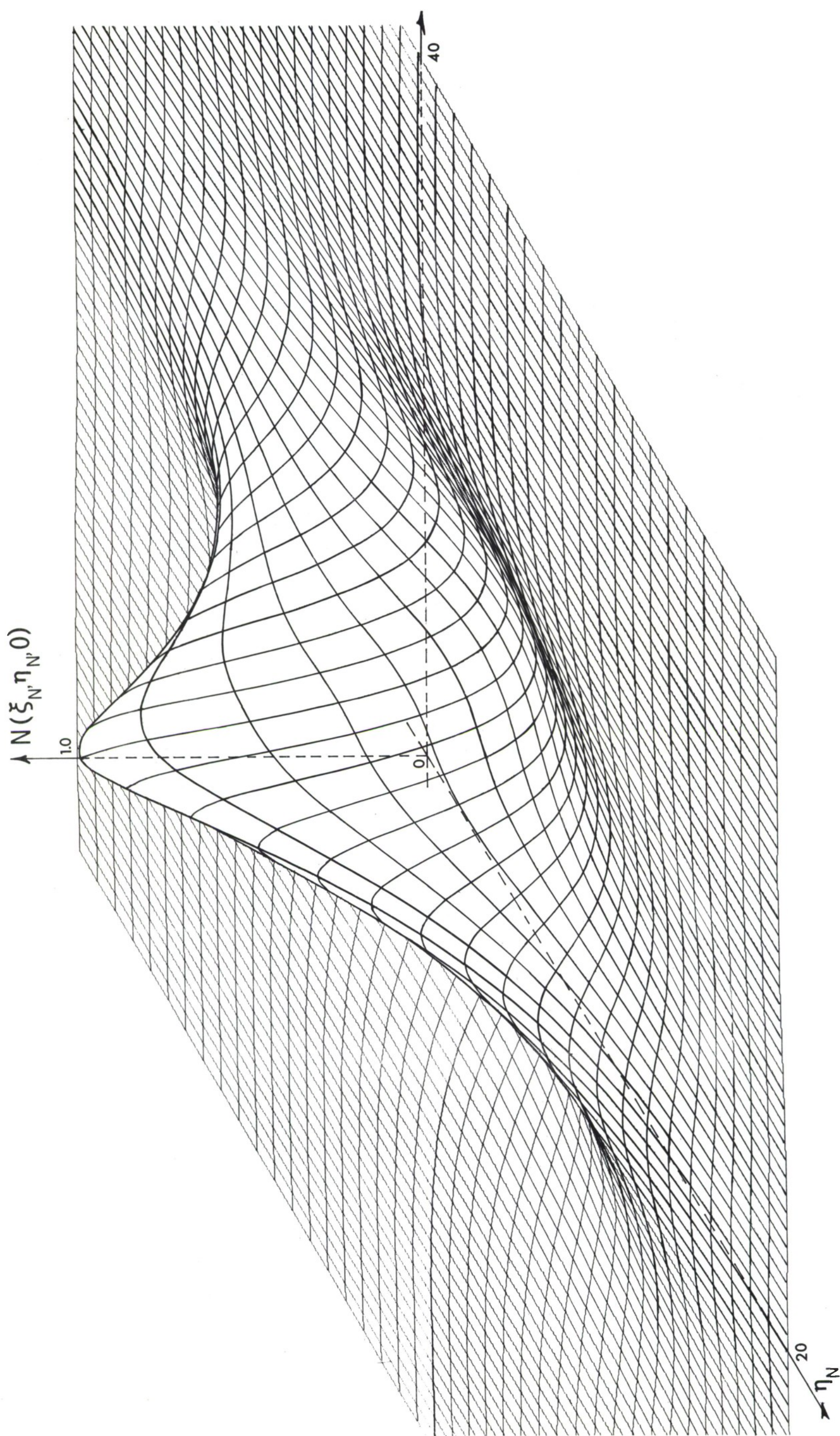


FIG. 4 SPATIAL CORRELATION FUNCTION OF WIND-GENERATED OCEAN SURFACE WAVES, DERIVED FROM THE NEUMANN SPECTRUM
The normalized correlation distances are $2g/U^2$ times the actual distance. ξ_N is the downwind direction, η_N the crosswind direction.

4.3 The Pierson-Moskowitz Spectrum

Now the variable σ is changed to z by means of the relation

$$z = \beta(\sigma_0/\sigma)^4, \quad [\text{Eq. 65}]$$

as in Sect. 3.3. Substitution of Eqs. 22, 36 and 58 into Eq. 56 gives expressions similar to Eqs. 61 and 62:

$$N(\xi_N, \eta_N, 0) = \rho_N^{-2} [\xi_N^2 L_1(\rho_N) + (\eta_N^2 - \xi_N^2) L_2(\rho_N)], \quad [\text{Eq. 66}]$$

$$N(\rho_N, \varphi, 0) = \cos^2 \varphi L_1(\rho_N) + (\sin^2 \varphi - \cos^2 \varphi) L_2(\rho_N); \quad [\text{Eq. 67}]$$

the functions L_1 and L_2 are defined as follows:

$$L_1(\rho_N) = 2 \int_0^\infty dz e^{-z} J_0\left(\frac{1}{2} \rho_N \beta^{\frac{1}{2}} z^{-\frac{1}{2}}\right) \quad [\text{Eq. 68a}]$$

$$L_2(\rho_N) = 2 \int_0^\infty dz e^{-z} J_1\left(\frac{1}{2} \rho_N \beta^{\frac{1}{2}} z^{-\frac{1}{2}}\right) / \left(\frac{1}{2} \rho_N \beta^{\frac{1}{2}} z^{-\frac{1}{2}}\right). \quad [\text{Eq. 68b}]$$

The results of the numerical calculation of L_1 and L_2 are presented in Fig. 5 and Table 2. Knowledge of these functions is sufficient to simplify the calculation of N from Eqs. 66 or 67. Figure 6 gives an impression of the surface $N(\xi_N, \eta_N, 0)$ for the Pierson-Moskowitz spectrum.

4.4 Down-Wind and Cross-Wind Correlation

From Figs. 4 and 6, the function $N(\xi_N, \eta_N, 0)$ can only be studied qualitatively, because these figures try to depict a three-dimensional surface in a two-dimensional plane. It is therefore worth considering two cross-sections of $N(\xi_N, \eta_N, 0)$, namely the down-wind correlation function $N(\xi_N, 0, 0)$ and the cross-wind correlation function $N(0, \eta_N, 0)$. Formulae for these functions are readily obtained from Eqs. 61 and 66:

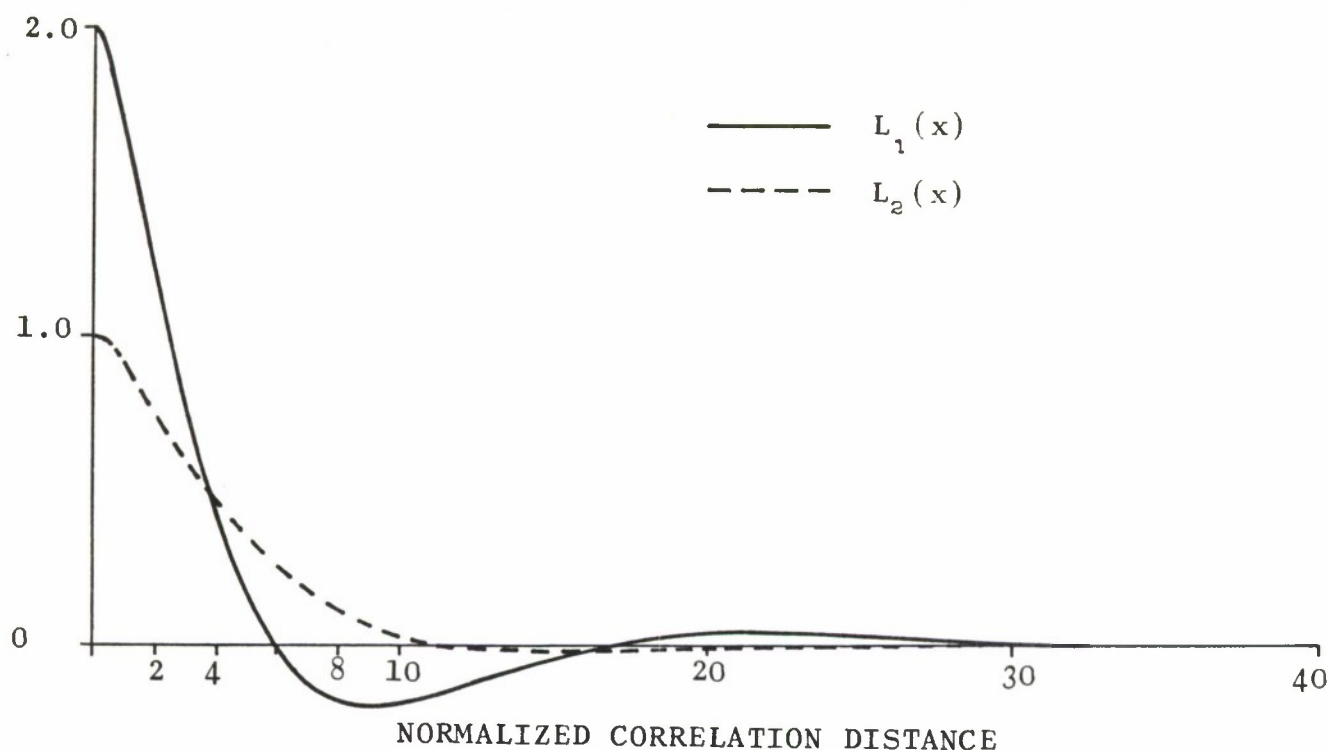


FIG. 5 THE FUNCTIONS $L_1(x)$ AND $L_2(x)$

x	$L_1(x)$	$L_2(x)$
0	2.000000	1.000000
1	1.685109	0.910138
2	1.207823	0.760491
3	0.765871	0.606300
4	0.410755	0.466143
5	0.150207	0.346600
6	-0.025481	0.248841
7	-0.132343	0.171491
8	-0.186940	0.112086
9	-0.203925	0.067769
10	-0.195557	0.035761
11	-0.172261	0.013510
12	-0.141542	-0.001208
13	-0.108166	-0.010259
14	-0.075907	-0.015168
15	-0.046841	-0.017151
16	-0.022416	-0.017162
17	-0.002859	-0.015920
18	0.011061	-0.013957
19	0.020852	-0.011660
20	0.028004	-0.009303
21	0.031476	-0.007071
22	0.031200	-0.005058
23	0.029420	-0.003309
24	0.027955	-0.001871
25	0.023396	-0.000733
26	0.019119	0.000152
27	0.016490	0.000777
28	0.010976	0.001198
29	0.008360	0.001459
30	0.004846	0.001557
31	0.001924	0.001578
32	0.000640	0.001495
33	-0.002759	0.001378
34	-0.002500	0.001215
35	-0.003234	0.001042
36	-0.003968	0.000861
37	-0.003838	0.000684
38	-0.003708	0.000518
39	-0.003743	0.000369
40	-0.003778	0.000237

TABLE 2 SAMPLE VALUES OF L_1 AND L_2

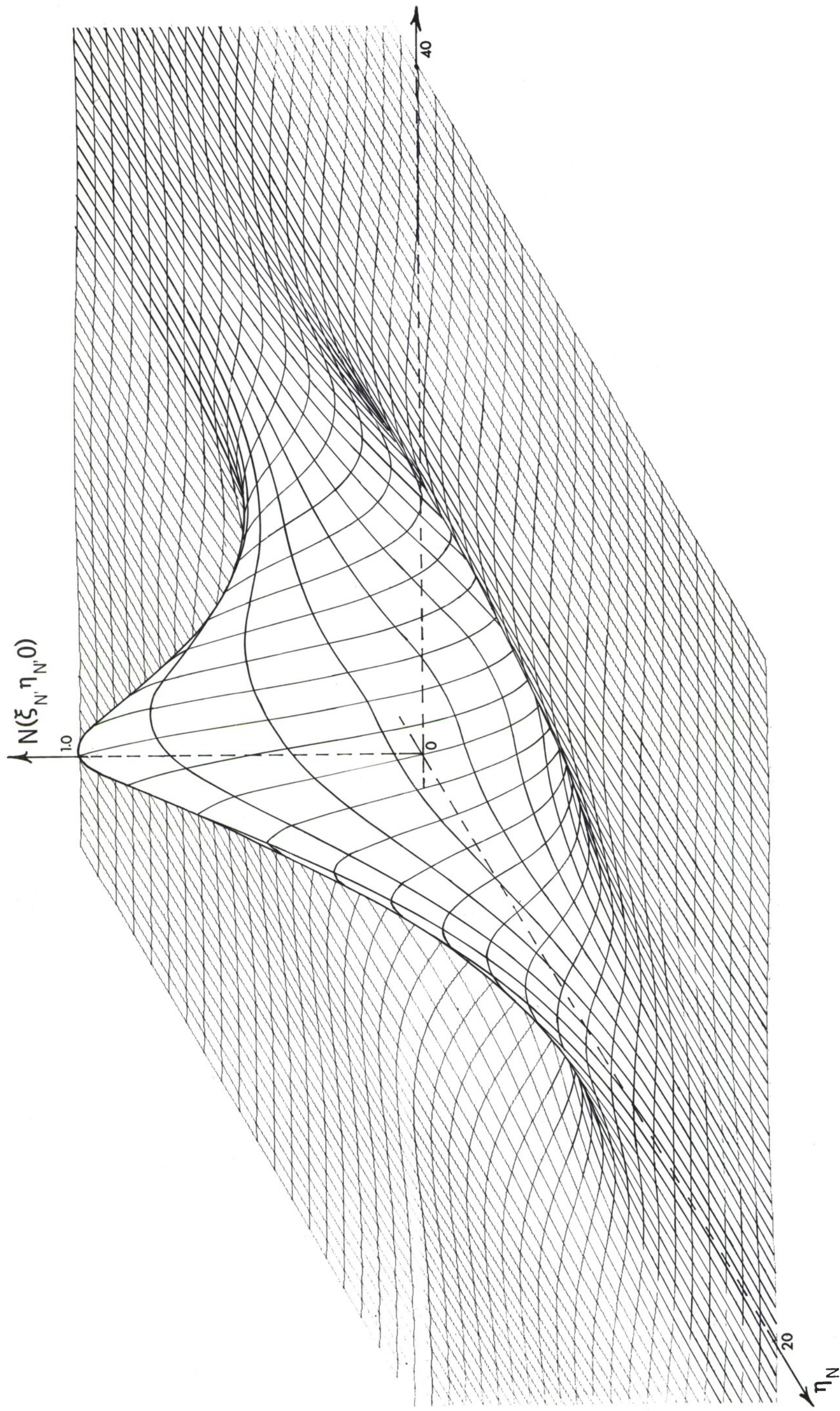


FIG. 6 SPATIAL CORRELATION FUNCTION OF WIND-GENERATED OCEAN SURFACE WAVES, DERIVED FROM THE PIERSON-MOSKOWITZ SPECTRUM
The normalized correlation distances are $2g/U^2$ times the actual distance. ξ_N is the downwind direction, η_N the crosswind direction.

a) Neumann Spectrum

$$N(\xi_N, 0, 0) = K_1(\xi_N) - K_2(\xi_N) \quad [\text{Eq. 69a}]$$

$$N(0, \eta_N, 0) = K_2(\eta_N) . \quad [\text{Eq. 69b}]$$

b) Pierson-Moskowitz Spectrum

$$N(\xi_N, 0, 0) = L_1(\xi_N) - L_2(\xi_N) \quad [\text{Eq. 70a}]$$

$$N(0, \eta_N, 0) = L_2(\eta_N) . \quad [\text{Eq. 70b}]$$

The corresponding curves and the difference between them are presented in Figs. 7 and 8. We note that the correlation in the cross-wind-direction [Fig. 8] is better than in the down-wind direction [Fig. 7].

4.5 Discussion

The difference between the spatial correlation functions obtained from the two energy spectra under study is difficult to see from a comparison between Figs. 4 and 6. This difference is therefore plotted in Fig. 9.

A more quantitative idea about the differences can be obtained from Figs. 7 and 8. The maximum value turns out to be about 0.1226, occurring at $\xi_N = 5$, $\eta_N = 0$.

The fact that the correlation distance could be normalized with respect to the wind speed confirms the conclusion reached for the time-correlation function, namely that the fully-developed sea changes only its scale, and not its shape, when the wind speed is changed and a new equilibrium is found.

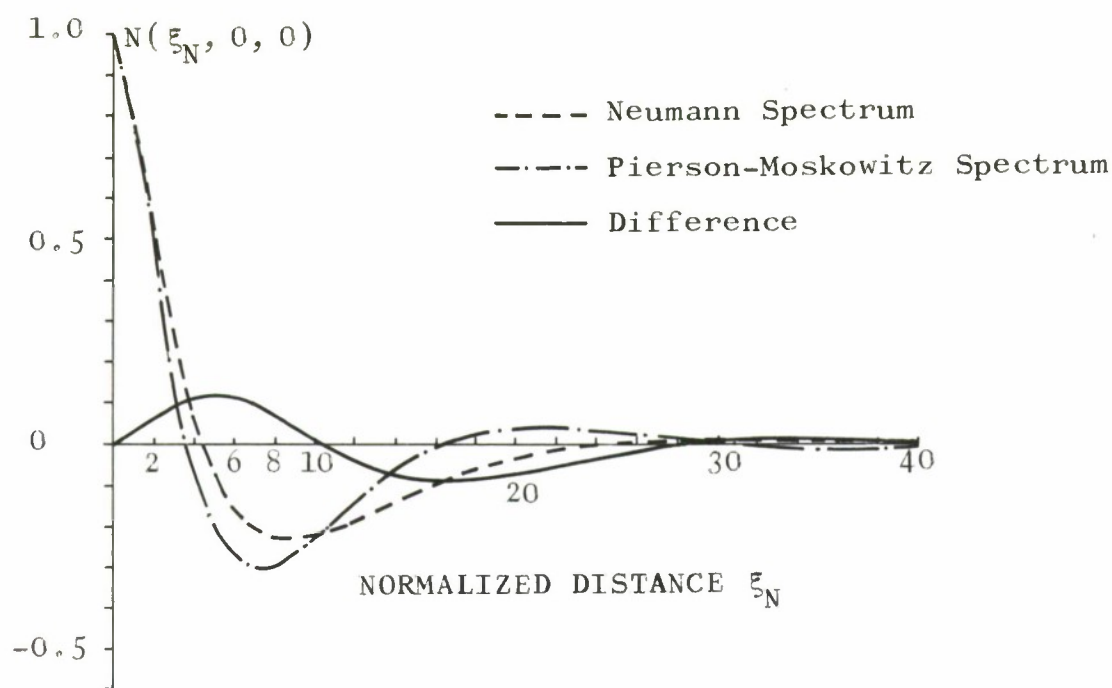


FIG. 7 SPATIAL CORRELATION FUNCTION OF WIND-GENERATED OCEAN SURFACE WAVES IN THE DOWN-WIND DIRECTION
The normalized distance equals $2g/U^2$ times the actual distance

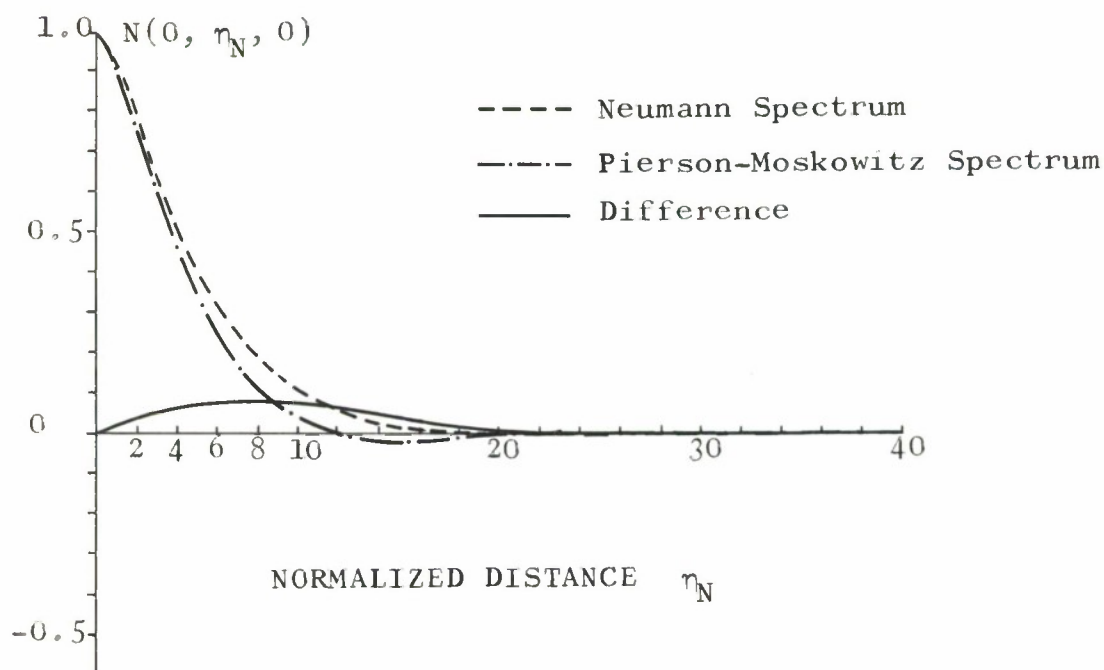


FIG. 8 SPATIAL CORRELATION FUNCTION OF WIND-GENERATED OCEAN SURFACE WAVES IN THE CROSS-WIND DIRECTION
The normalized correlation distance equals $2g/U^2$ times the actual distance.

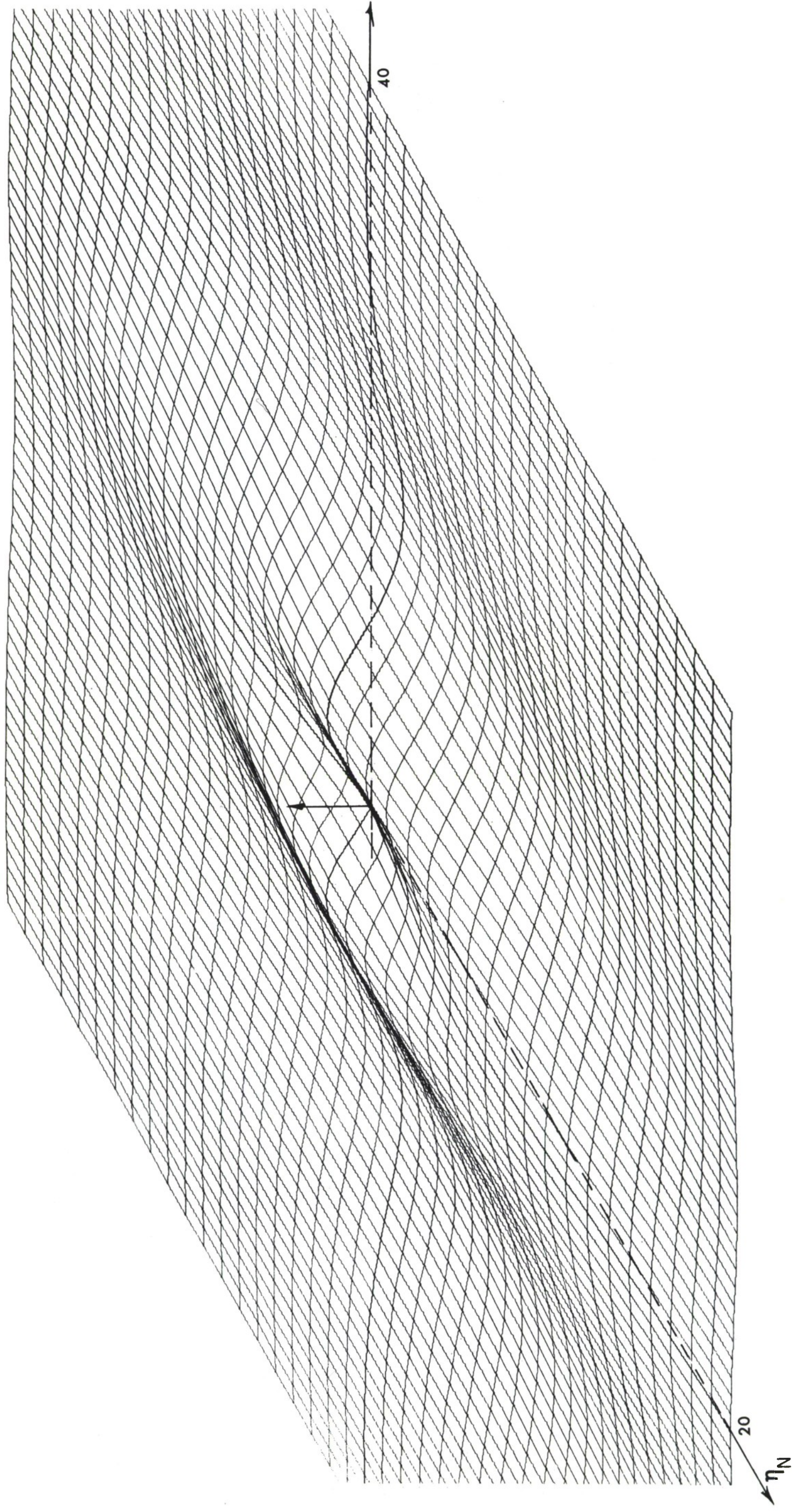


FIG. 9 THE DIFFERENCE BETWEEN THE SPATIAL CORRELATION FUNCTIONS OF WIND-GENERATED OCEAN WAVES, OBTAINED FROM THE NEUMANN AND THE PIERSON-MOSKOWITZ SPECTRA

CONCLUSIONS

Wind-generated sea surface waves can be considered with good approximation as a Gaussian process $\zeta(\vec{x}, t)$, stationary in time, and homogeneous and anisotropic in space. If the mean value of this process is set equal to zero, which can be done without loss of generality, the correlation function

$$h^2 N(\vec{\rho}, \tau) = E[\zeta(\vec{x}, t) \zeta(\vec{x} + \vec{\rho}, t + \tau)]$$

represents the process completely in a statistical sense. This correlation function plays an important role in the description of an underwater sound field that is scattered from the sea surface.

The most realistic way to describe the surface waves statistically is by using a surface wave energy spectrum $\Phi(\sigma, \theta)$. The correlation function $N(\vec{\rho}, \tau)$ is related to the energy spectrum through a double Fourier integral, over wave frequency and wave direction. The time-correlation function follows with $\vec{\rho} = 0$, the spatial-correlation function with $\tau = 0$. For two proposed spectral functions for fully-developed seas, the Neumann and the Pierson-Moskowitz spectra, we have calculated the correlation functions $N(0, \tau)$ and $N(\vec{\rho}, 0)$ on a digital computer. It turned out, as was already indicated by Pierson and Moskowitz, who normalized the wave frequency and the fetch, that the scales could be normalized with respect to the wind speed: normalized time equals real time divided by wind speed; normalized distance is proportional to real distance divided by the square of the wind speed. This indicates that two fully-developed seas of infinite fetch, with different constant wind speeds, differ only in scale, and not in shape.

As the Neumann and Pierson-Moskowitz spectra are only given as functions of wave frequency σ , but not of wave direction θ ,

a relation between the directional spectrum and its isotropic mate had to be assumed. We have chosen the frequently met $(\cos^2 \theta)$ -connection, but a more adequate relation might be given by using $\cos^p \theta$, where p is frequency-dependent.

Although the correlation function $N(\vec{\rho}, 0)$ is essentially a function in two dimensions, it could be expressed in two functions that depend only on the modulus of $\vec{\rho}$. This is an important result for the description of the underwater scattered sound field when it comes to numerical evaluation of its statistical properties: instead of having to represent $N(\vec{\rho}, 0)$ as a matrix of $M \times M$ elements, two column vectors of size M will suffice. A simple calculation then yields $N(\vec{\rho}, 0)$ for each spatial point. Sample values of these two functions are included in this report, for $M = 40$.

It is found that the Neumann and Pierson-Moskowitz spectra produce correlation functions that differ only quantitatively.

APPENDIX A

TOTAL ENERGY IN A FULLY DEVELOPED SEA

The total energy E is defined by Eq. 28:

$$E = \int_0^{\infty} d\sigma \Phi(\sigma). \quad [\text{Eq. A.1}]$$

We shall now derive Eqs. 29 and 30.

a) Neumann Spectrum

Substitution of Eq. 16 into Eq.A.1 gives:

$$E = C \frac{\pi}{2} \int_0^{\infty} d\sigma \sigma^{-6} \exp(-2g^2/\sigma^2 U^2), \quad [\text{Eq. A.2}]$$

and with

$$z = g \sqrt{2}/\sigma U \quad [\text{Eq. A.3}]$$

this becomes

$$E = C \frac{\pi}{2} \left(\frac{U}{g \sqrt{2}} \right)^5 \int_0^{\infty} dz z^4 e^{-z^2}. \quad [\text{Eq. A.4}]$$

The integral has the value $\frac{3}{8} \sqrt{\pi}$, which has been found in Ref. 9 [p.337, no.(3.461.2)]. And so we have finally

$$E = 3C \left(\frac{\pi}{2} \right)^{3/2} \left(\frac{U}{2g} \right)^5. \quad [\text{Eq. A.5}]$$

b) Pierson-Moskowitz Spectrum

We substitute Eq. 22 into Eq. A.1, and find:

$$E = \alpha g^2 \int_0^{\infty} d\sigma \exp \left[-\beta \left(\frac{\sigma_0}{\sigma} \right)^4 \right] \sigma^{-5}. \quad [\text{Eq. A.6}]$$

With the change of variables

$$z = \beta \left(\frac{\sigma}{\sigma_0} \right)^4 \quad [\text{Eq. A.7}]$$

Eq. A.6 reduces to

$$E = \frac{1}{4} \frac{\alpha}{\beta} \frac{g^2}{\sigma_0^4} \int_0^\infty dz e^{-z} = \frac{\alpha g^2}{4\beta \sigma_0^4} , \quad [\text{Eq. A.8}]$$

or, because of $\sigma_0 = g/U$,

$$E = \frac{4\alpha g^2}{\beta} \left(\frac{U}{2g} \right)^4 . \quad [\text{Eq. A.9}]$$

APPENDIX B

CALCULATION OF THE INTEGRAL $I_1(\sigma, \vec{\rho})$

We call φ the angle made by the vector $\vec{\rho}$ with the ξ -axis.
So we have:

$$\sin \varphi = \eta / \rho, \quad \cos \varphi = \xi / \rho. \quad [\text{Eq. B.1}]$$

Hence Eq. 57 can be written as

$$I_1(\sigma, \vec{\rho}) = \int_{-\pi/2}^{\pi/2} d\theta \cos^2 \theta \cos[\rho' \cos(\theta - \varphi)], \quad [\text{Eq. B.2}]$$

where $\rho' = \sigma^2 \rho / g$.

Next we introduce the new variable $\theta' = \theta - \varphi$, and drop the prime. Then we obtain

$$I_1(\sigma, \vec{\rho}) = \int_{-\pi/2-\varphi}^{\pi/2-\varphi} d\theta \cos^2(\theta + \varphi) \cos(\rho' \cos \theta), \quad [\text{Eq. B.3}]$$

and with the identity

$$\cos^2(\theta + \varphi) = \cos^2 \theta \cos^2 \varphi + \sin^2 \theta \sin^2 \varphi - \frac{1}{2} \sin(2\theta) \sin(2\varphi) \quad [\text{Eq. B.4}]$$

I_1 can be split into three parts:

$$\begin{aligned} I_1(\sigma, \vec{\rho}) &= \cos^2 \varphi \int_{-\pi/2-\varphi}^{\pi/2-\varphi} d\theta \cos^2 \theta \cos(\rho' \cos \theta) \\ &+ \sin^2 \varphi \int_{-\pi/2-\varphi}^{\pi/2-\varphi} d\theta \sin^2 \theta \cos(\rho' \cos \theta) \\ &- \frac{1}{2} \sin(2\varphi) \int_{-\pi/2-\varphi}^{\pi/2-\varphi} d\theta \sin(2\theta) \cos(\rho' \cos \theta). \end{aligned} \quad [\text{Eq. B.5}]$$

The three integrands have the period π , because $\cos^2 \theta$, $\sin^2 \theta$, $\sin(2\theta)$ and $\cos(\rho' \cos \theta)$ have that period. And since we have to integrate over an interval of length π , we can take the limits from $-\pi/2$ to $+\pi/2$. But then the third integral vanishes, as the integrand is odd. And the value of the two remaining integrals is not changed if we integrate from 0 to π , instead of from $-\pi/2$ to $+\pi/2$. Hence, we have:

$$I_1(\sigma, \vec{\rho}) = \cos^2 \varphi \int_0^\pi d\theta \cos^2 \theta \cos(\rho' \cos \theta) + \sin^2 \varphi \int_0^\pi d\theta \sin^2 \theta \cos(\rho' \cos \theta). \quad [\text{Eq. B.6}]$$

Substitution of $\cos^2 \theta = 1 - \sin^2 \theta$ gives

$$I_1(\sigma, \vec{\rho}) = \cos^2 \varphi \int_0^\pi d\theta \cos(\rho' \cos \theta) + (\sin^2 \varphi - \cos^2 \varphi) \int_0^\pi d\theta \sin^2 \theta \cos(\rho' \cos \theta). \quad [\text{Eq. B.7}]$$

The integrals are readily evaluated with tables [see Ref. 9, pp.402-403, nos.18 and 21]:

$$I_1(\sigma, \vec{\rho}) = \pi \left[\cos^2 \varphi J_0(\rho') + (\sin^2 \varphi - \cos^2 \varphi) \frac{J_2(\rho')}{\rho'} \right]. \quad [\text{Eq. B.8}]$$

With Eq. B.1 and $\rho' = \sigma^2 p/g$ into this formula, Eq. 58 follows.

REFERENCES

1. L. Fortuin, "A Survey of Literature on Scattering and Reflection of Sound Waves from Rough Surfaces", SACLANTCEN Technical Report No. 138, February 1969, NATO UNCLASSIFIED.
2. B. Kinsman, "Wind Waves, their Generation and Propagation on the Ocean Surface", Prentice-Hall, Englewood Cliffs, N.J., 1965.
3. O.M. Phillips, "The Dynamics of the Upper Ocean", University Press, Cambridge, 1966.
4. M. Schulkin, "The Propagation of Sound in Imperfect Ocean Surface Ducts", USL Report No. 1013, April 1969.
5. W.J. Pierson, and L. Moskowitz, "A Proposed Spectral Form for Fully Developed Wind Seas Based on the Similarity Theory of S.A. Kitaigorodskii", J. Geophys. Res., Vol. 69, No. 24, pp.5181-5190, 1964.
6. G.E. Latta, and J.A. Bailie, "On the Autocorrelation Functions of Wind Generated Ocean Waves", Zeitschrift Angewandte Mathematik und Physik, Vol. 19, pp.575-586, 1968.
7. J.S. Bendat, "Spectra and Autocorrelation Functions for Fully Developed Seas and Prediction of Structural Fatigue Damage", Measurement Analysis Corporation, Report No. 307-04, September 1964.
8. D. Stilwell, "Directional Energy Spectra of the Sea from Photographs", J. Geophys. Res., Vol. 74, No. 8, pp.1974-1986, 1969.
9. I.S. Gradshteyn and I.M. Ryzhik, "Table of Integrals Series and Products", Academic Press, New York/London, 1965.

DISTRIBUTION

	Copies		Copies
<u>MINISTRIES OF DEFENCE</u>		<u>SCNR for SACLANTCEN</u>	
MOD Belgium	5	SCNR Belgium	1
MOD Canada	10	SCNR Canada	1
MOD Denmark	10	SCNR Denmark	1
MOD France	8	SCNR Germany	1
MOD Germany	13	SCNR Greece	1
MOD Greece	11	SCNR Italy	1
MOD Italy	8	SCNR Netherlands	1
MOD Netherlands	10	SCNR Norway	1
MOD Norway	10	SCNR Turkey	1
MOD Portugal	5	SCNR U.K.	1
MOD Turkey	3	SCNR U.S.	1
MOD U.K.	20		
SECDEF U.S.	71		
		<u>NATIONAL LIAISON OFFICERS</u>	
<u>NATO AUTHORITIES</u>		NLO Italy	1
North Atlantic Council	3	NLO Portugal	1
NAMILCOM	2	NLO U.K.	1
SACLANT	3	NLO U.S.	1
SACEUR	3		
CINCHAN	1	<u>NLR to SACLANT</u>	
SACLANTREPEUR	1	NLR Belgium	1
COMNAVSOUTH	1	NLR Canada	1
CINCEASTLANT	1	NLR Denmark	1
COMMAIREASTLANT	1	NLR Germany	1
COMCANLANT	1	NLR Greece	1
COMOCEANLANT	1	NLR Italy	1
COMEDCENT	1	NLR Norway	1
COMSUBACLANT	1	NLR Portugal	1
COMSUBEASTLANT	1	NLR Turkey	1
COMMARAIRMED	1		
COMSTRIKFORSOUTH	1	ESRO/ELDO Doc. Serv.	1
COMSUBMED	1		